Towards functional restoration for persons with limb amputation: A dual-stage implementation of regenerative agonist-antagonist myoneural interfaces

Shriya S. Srinivasan, BS.[1,2], Maurizio Diaz[2], Matthew Carty, MD[3], Hugh M. Herr*, PhD[2]

[1]Harvard-MIT Division of Health Sciences and Technology, Massachusetts Institute of Technology, Cambridge, MA 02139, USA; correspondence: shriyas@mit.edu
[2]Center for Extreme Bionics, MIT Media Lab, Massachusetts Institute of Technology, Cambridge, MA 02139, USA.
[3]Department of Plastic and Reconstructive Surgery, Brigham and Women's Hospital, Boston, MA 02115, USA.
*Correspondence can be sent to hherr@media.mit.edu

While amputation has traditionally been viewed as a failure of therapy, recent developments in amputation surgery and neural interfacing demonstrate improved functionality and bidirectional communication with prosthetic devices. The agonist antagonist myoneural interface (AMI) is one such bi-directional neural communication model comprised of two muscles, an agonist and an antagonist, surgically connected in series within the amputated residuum so that contraction of one muscle stretches the other. By preserving agonist-antagonist muscle dynamics, the AMI allows proprioceptive signals from mechanoreceptors within both muscles to be communicated to the central nervous system. Preliminary human evidence suggests that AMIs have the capacity to provide high fidelity control of a prosthetic device, force feedback, and natural proprioception. However, AMIs have been implemented only in planned amputations and requires healthy distal tissues, whereas the majority of amputations occur in patients who do not have healthy distal tissues. Through the use of a dual-stage surgical procedure which leverages existent tissues, this study proposes a revision model for implementation of the AMI in patients who are undergoing traumatic amputation or have already undergone a standard amputation. This paper validates the resulting AMI's physiology, revealing robust viability and mechanical and electrophysiological function. We demonstrate the presence of H-waves in regenerative grafts, indicating the incorporation of the AMI into physiological reflexive loops.

Introduction

Limb amputation is generally perceived as a failure of therapy, instead of an opportunity to provide functional restoration. The traditional approach to extremity amputation suffers from a lack of sophisticated options

for patients and results in residual limbs that are frequently complicated by secondary pathologies. Common negative sequelae include bone spurs (14-56%), soft tissue pathology (15-24%), neuroma formation (18-38%), and ulceration (6-31%)[1–3]. These issues, in addition to poor stump formation, often become prohibitive to wearing and controlling prostheses and thereby limit motor function. Consequently, there is an alarmingly high rate of revision for amputation, reported between 5-30% for lower extremity (below-knee or above-knee) amputation[4].

However, with current biomechatronics and robotic technologies, combined with progressing surgical techniques, we are stepping into an era in which the residual limb can be crafted with specific dynamic, sensory and motor components to facilitate a smooth transition to a functionally advanced state. Cross-disciplinary work between the biomechatronics and surgery fields has led to the creation of new amputation surgical procedures incorporating neural interfaces through which myoelectric prostheses can be controlled. For example, targeted muscle reinnervation (TMR), regenerative peripheral nerve interfaces (RPNIs), and agonist-antagonist myoneural interfaces (AMIs) address the challenge of deriving stable, high signal-to-noise ratio signals from muscles[5–7].

AMIs specifically restore dynamically functional neuromuscular constructs to residual limbs and enable natural musculotendinous proprioception by linking agonist-antagonist paired muscles within the amputated residuum[7]. In this configuration, when the user volitionally contracts an agonist muscle, the antagonist muscle undergoes stretch. Length and force information from the antagonist muscle, critical for joint stability, fine motor control, and trajectory planning, are conveyed to the central nervous system through afferent signaling pathways[8]. When paired with a myoelectric prosthetic device, force, state, and impedance information from the AMI can be conveyed to control prosthetic joints with high fidelity[9]. Functional electrical stimulation (FES) can be employed to provide feedback to the AMI regarding the prosthesis' position, state, and impedance[9]. Each muscle of the AMI can be independently stimulated based on parameters calculated from a biophysical model using state, force and impedance data acquired from the AMI. This will enable communication of prosthetic movement, whether the joint is moving or locked in position under varying torques. As a result, the AMI establishes a bidirectional signaling capacity between an amputated residuum and a prosthetic device. In murine studies, regenerative AMIs have demonstrated robust efferent and afferent signaling and strains that graded with stimulation amplitude[7,10]. Further, one patient has undergone the surgical creation of an AMI during a planned amputation. In functional testing, this patient outperformed control patients with standard amputation on tasks requiring proprioception[9].

Multiple AMIs can be created within a residual limb, one for each degree of freedom (DOF) desired in the corresponding prosthetic device. For planned amputations where sufficient distal musculature is healthy and available, AMIs can be constructed by linking the agonist-antagonist muscle pairs associated with the amputated joint through a synovial canal inside the residual limb. However, in the majority of patients requiring amputation, distal tissues are not healthy and/or available for use (in cases of pathology or trauma ~90%). In these cases, the AMI can be constructed using regenerative muscle grafts harvested from a donor site on the same patient. These grafts can be neurotized with transected extensor-flexor pair nerves and linked in agonist-antagonist pairs. Regenerative AMIs demonstrated a time course of maturation compatible with atrophy, neural plasticity, and scarring[7].

Because the regenerative AMI approach does not require large, healthy, native muscles, it is especially robust. Once implemented during a revision operation in patients who have already undergone amputation, it may provide newfound capabilities for myoelectric prosthesis control. The small footprint of each graft (4cm x 1cm) enables the method to scale to multiple DOFs. Coupled with the benefit of potentially facilitating advanced motor capabilities through high fidelity control of sophisticated prostheses, implementation of the AMI in revision amputees may also provide the benefit of neuroma ablation and the potential to sustain muscle bulk due to hypertrophy from volitional use of those muscles.

For the aforementioned advantages, regenerative AMIs would be a substantial improvement towards the functional restoration of amputated residua. However, their surgical construction requires the knowledge of the identity/function of each anatomically relevant nerve. Unlike a *de novo* amputation, a revision surgery procedure is constrained by the tissues in the stump and their structure, as created during the initial amputation. Given the variety of amputation procedures commonly practiced, nerves are often transected at non-standardized locations and may be found buried inside or between muscles or lodged inside bone. Often, they also form neuromas, making the identification of each fascicle very challenging. This study addresses the nuanced challenge of constructing AMIs using regenerative muscle grafts in a revision procedure by proposing and validating a surgical strategy to overcome the difficulty of proper nerve identification.

Following amputation, neuromas are formed in 13-36% of patients, can inflict pain a month after transection, and are one of the most predominant reasons for revision surgery. Whilst most neuromas form as bulbous focal lesions, a majority of them also contain irregular fibers that regenerate in various directions and

complicate their isolation. After encapsulation by perivascular tissue, neuromas sprout axons that intertwine and adhere to surrounding tissues[11]. Repeated weight bearing leads to inflammation and irritation, resulting in drastic hyperproliferation (10+ times original) and disorganized morphologies[11,12].

In procedures like TMR and RPNI, the neuroma is removed surgically[13] and the transected nerve branches are placed in nearby or grafted muscles. Identification of the function and/or target muscle of each nerve is not required, since each nerve innervates one isolated end-target muscle that remains independent of other end-target activation. However, in the case of the AMI, it is necessary to identify the flexor and extensor pairs in order to connect the appropriate grafts and establish proxy joints. Practically, the complex and variable topographical organization of large nerves, compounded by nerve healing and scarring, often makes it challenging to identify specific fascicles, especially at higher levels of amputation.

For instance, the sciatic nerve, is composed of ten major branches, comprising five different flexor-extensor pairs. Efferent activation of the peroneal nerves contracts the tibialis muscle, causing *dorsiflexion* of the ankle joint, while the gastrocnemius undergoes *extension* and transmits afferent signals through the tibial nerve. Though, in principle, the peroneal and tibial nerves could be identified by size and anatomy, after amputation and potential neuroma formation it is often difficult to identify and isolate them with certainty. Lack of definitive nerve flexor-pair identification precludes the construction of AMIs reflecting the DOFs of each joint.

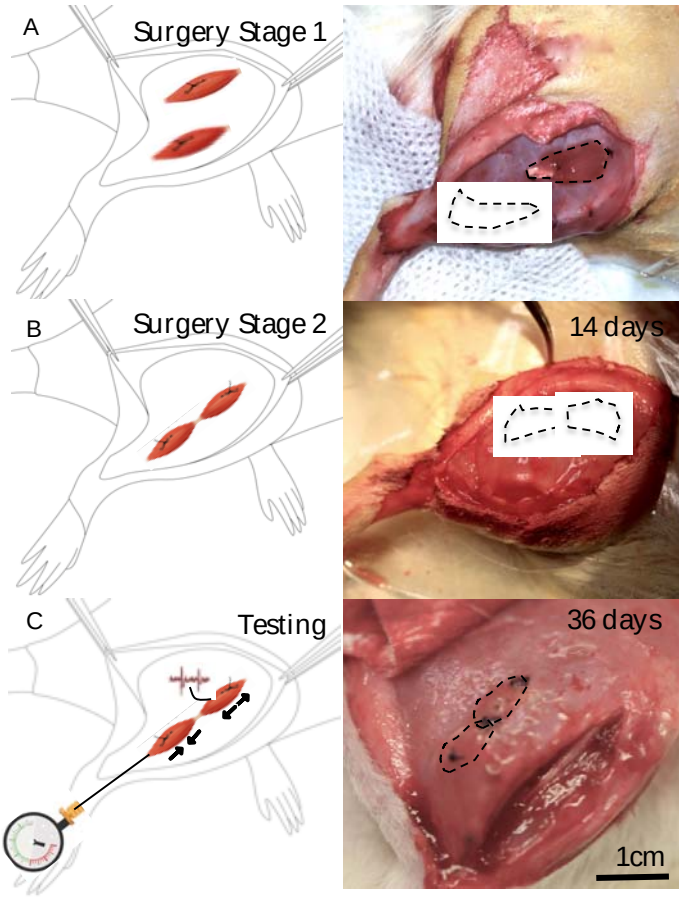

Figure 1. Dual-Stage Regenerative AMI Procedure. A) In the first stage of surgery, two separate regenerative muscle grafts (circumscribed by dotted lines) innervated with the tibial and peroneal nerves are created and placed on the biceps femoris. B) During the second surgical stage, grafts are lifted from their original sites, coapted by their tendons to form an AMI, and sutured to fascia at the same tension. C) After 5 weeks, electrophysiological, histological, and mechanical testing is performed. Under stimulation, the agonist graft contracts while the antagonist undergoes extension. Figure based on original artwork by Stephanie Ku.

Dual-stage surgical model

In this study, we design a dual-stage surgical approach to overcome the challenges related to proper identification of transected nerves and construct AMIs for any revision patient. A detailed flowchart outlining an example case in which the surgery would be performed is provided in the supplemental information (Supplemental Figure. 1). Briefly, in the first stage, each terminal nerve in the residual limb would be dissected to the fascicular level and sutured into muscle grafts. These grafts would be placed in close proximity to the predicted antagonist graft. After reinnervation, the patient would be instructed to volitionally contract each muscle graft and identify its motor function. We can also perform ultrasound-guided electrical stimulation of the grafts and ask patients to report the sensed muscle. Each muscle graft would then be tagged using anatomical landmarks or injected fluoroscopic markers. During a second surgery, the appropriate flexor-extensor pairs would be connected to form AMIs. Any grafts that cannot be identified or do not have a clear extensor or flexor function will be left unlinked.

This approach however, involves, interrupting the process of reinnervation and revascularization and generation of additional scarbeds upon free muscle grafts, potentially jeopardizing their viability and dynamic functionality (ability to contract/extend), which is essential to the generation of musculotendinous mechanotransduction - the foundation of the AMI. Therefore, in this study, we evaluate the ability of the AMI to be formed and function using a dual-stage surgical process, overcoming the effects of additional scarring and a disrupted vascular bed.

We hypothesize that a dual-stage surgery will not mitigate critical functional components of the AMI including reinnervation, tissue health, atrophy and strain when compared to a single-stage AMI (positive control). We hypothesize that forces produced by the AMI will grade with stimulation amplitude. Additionally, we anticipate that regenerative AMI grafts will generate afferent signals and electrophysiological reflex arcs consistent with stimulation amplitude and mitigate atrophy when compared to unlinked grafts (negative control). To evaluate these hypotheses, we construct AMIs in murine models (n=5) using single and dual stage methods. We also create a negative control group (n=5) in which regenerative grafts are not linked to form AMIs to investigate the effect of agonist-antagonist pairing on the prevention of atrophy. Five weeks post-operatively, we perform electrophysiological, mechanical and histological studies to evaluate our hypotheses.

Methods:

All animal experiments were conducted under the supervision and approval of the Committee on Animal Care at the Massachusetts Institute of Technology (MIT) in accordance with the relevant guidelines and regulations on male Lewis rats (n = 13, weight range: 302—309g) under 1- 2.5% isoflurane used for anesthesia. The experimental (n=5) and positive control groups (n=5) underwent AMI construction in a dual-stage and single-stage method, respectively. Additionally, in a negative control group (n=5), unlinked neuromuscular grafts were created to assess effects of atrophy and afferent signaling in the absence of an antagonist pair.

Surgical procedure: In stage one, a curvilinear incision was performed on the right hind limb to expose the anterior and posterior muscle groups. Following partial reflection of the biceps femoris, the extensor digitorum longus muscle was isolated and disinserted. The weight and length of the muscle were measured. Myotomy of the extensor digitorum longus muscle created two equally sized muscle grafts. Muscle grafts were sutured to the superficial fascia of the biceps femoris (5-0 absorbable suture) and situated approximately one centimeter from each other. The tibial and common peroneal nerves were isolated and distally transected and elevated through slits in the biceps femoris. Their usage simulates that of any given flexor-extensor pair or two unknown fascicles in the human case. A superficial myotomy was performed through the epimysium of each muscle segment to neurotize with either the peroneal or tibial nerve (8-0 microsuture) and create two distinct muscle grafts (Figure 1A). The incision was closed using a 4-0 suture. Two weeks after the first surgery, we performed electromyography to confirm partial reinnervation. In the murine model, the innervating nerve of each graft was known. However, in the human implementation, electromyography would be performed to assess the function of each graft. Then, during a second surgery, blunt dissection of the scar bed surrounding each muscle was performed to mobilize the grafts. The tendinous regions of both grafts were linked using 4-0 nylon sutures to create an AMI.

Controls: For positive controls, AMIs were created out of regenerated muscle grafts in a single surgical step, as previously reported[7]. In negative controls, the second stage of surgery was not performed and muscle grafts remained isolated throughout (Supplemental Figure. 2).

Outcome Assessment: To assess reinnervation, insertional needle EMG was performed weekly as described previously[7]. Six weeks post-operatively, electrophysiology was performed to measure ENG and EMG from each nerve and muscle, respectively. Excursion, insertional activity, atrophy, coupled motion and strain were quantified as previously described[7]. Procedural details can be found in the supplemental information.

In dual-stage AMIs, the forces generated by the agonist graft were measured using a Shimpo FGV1XY 1lb

capacity digital force gauge. 4-0 nylon suture was sutured to the end of the agonist muscle and attached to the lever arm of the force gauge. The system was positioned such that a small non-zero force was registered on the system at baseline to ensure that no slack was present during the measurement.

Hematoxylin & eosin (H&E) and trichrome staining were performed to assess morphology, healing, revascularization, reinnervation, and fibrosis. Additionally, alpha bungarotoxin was used to stain for synaptogenesis and verify the extent of reinnervation. S46 binds to slow, tonic, myosin heavy chains and was used to stain intrafusal spindle fibers.

T-tests were used to compare the experimental and control groups to evaluate statistical significance. Prior work and comparable studies demonstrate normality in the measured metrics.

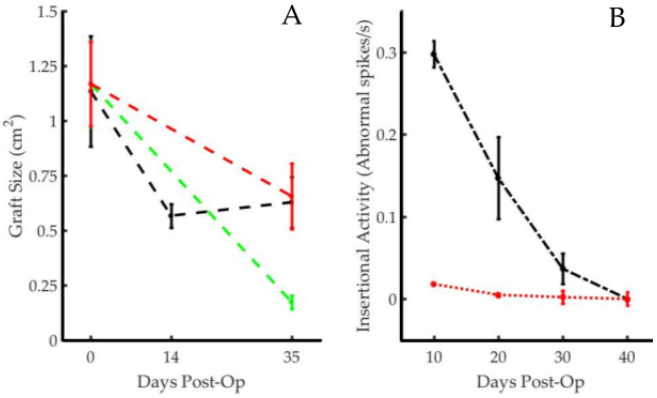

Figure 2. Reinnervation and Atrophy Trends. (A) Average graft size (n=5 each) and standard deviation at each surgical step or final testing session is shown; dual-stage AMIs (black), underwent similar rates of atrophy to single-stage AMIs (red) but were significantly less than the separated grafts (green). B) Insertional needle EMG activity levels in the dual-stage AMI (black) are compared to those in the contralateral gastrocnemius (red) (n=5).

Results

In all animals, AMIs were successfully created employing the peroneal and tibial nerve pair using a two-step surgical process. At terminal harvest, gross morphology indicated well-healed and revascularized grafts. No infection, graft failure, necrosis or ulceration occurred in any animals.

Atrophy: It is important to maintain muscle mass in AMIs, since it directly correlates with strength of efferent signal. For dual-stage AMIs, muscle atrophy occurred predominantly between stage one and stage two during the reinnervation and revascularization process (51 +/- 2.5% reduction in size). The average total atrophy at 35 days post-operatively was 41.62 +/- 3.2%. Between the creation of the AMI and the terminal harvest, animals demonstrated a 9.7 +/- 1.8% increase in graft size (Figureure 2A). Single-stage AMIs underwent 52 +/- 7.1% atrophy. The

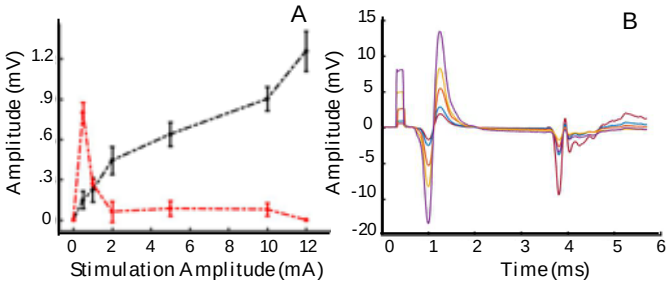

Figure. 3. M- and h-wave Trends. (A) Shown are average m-wave (black) and h-wave (red) amplitudes at each stimulation amplitude (0.5, 1, 2, 5, 10 mA). (B) Shown are average EMG amplitude of m and h waves in response to 100us, square stimulus pulse on the tibial nerve (n=150). As m-wave amplitude increases, h-wave amplitude decreases. (C) Electrophysiological set up to measure afferent signals generating from the antagonist due to agonist contraction. A stimulation pulse is applied to the agonist nerve while measuring ENG from the antagonist nerve to survey for afferent feedback signals. (D) Graded afferent signals correlated linearly with antagonist strain demonstrating that the agonist and antagonists grafts performed proportionally coupled excursion.

quantity of atrophy between the single-stage and dual-stage surgery groups was insignificant by a one-tailed 2-sample t test at p =.01. However, unlinked grafts experienced 87 ± 4.2% reduction in size, and were significantly smaller compared to linked AMIs at the p = .01 level (Supplemental Figure. 2).

Reinnervation was assessed through needle electrophysiology. The frequency of abnormal insertional activity decreased steadily and 35 days post-surgery, it was comparable to that of the contralateral gastrocnemius muscle (p <.001, 2-sample t-test) (Figure 2B). This result is comparable with previously published trends[7,14]. During the reinnervation process, end plate spikes, polyphasic motor unit potentials and fibrillation potentials commonly occurred.

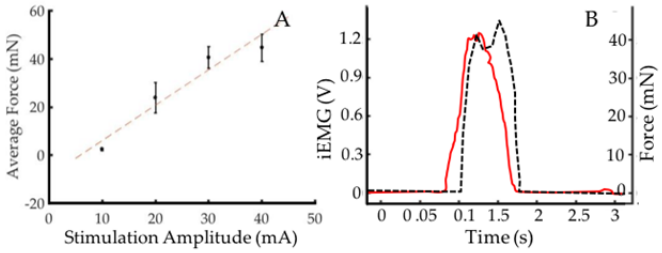

Figure 4. Regenerative AMI Force Production. (A) Forces produced by the muscles linearly scales as a function of stimulation amplitude. (B) Representative plot of iEMG (red) and force (dotted black) production shows physiologic excitation-contraction coupling delay.

Efferent and Afferent Signals: Strong, isolated, efferent electromyographic signals are required for the control of a prosthetic device. Using neural stimulation, isolated EMG signals were produced in each muscle graft, with no electrical leakage or inappropriate noise in the antagonist graft. The average signal to noise ratio for dual-stage grafts was 80.2, 84.0 for single-stage grafts, and 69.3 for unlinked grafts, which is sufficient for myoelectric prosthesis control[5]. Despite the scarring present, signals were isolated and produced a healthy biphasic trend. Thirty-five days post-operatively, muscles produced strong m-wave responses, and the compound muscle action potentials graded with stimulation amplitude (Figure 3A). In addition, h-waves were identified in 70% of the dual-stage AMI grafts (Figure 3B) during stimulation of the peroneal or tibial nerves. These responses were elicited at stimulation of 0.5 mA and decreased in magnitude through 5 mA. 10 mA stimulation did not elicit any h-waves in 8 of the 10 cases tested. Notably, h-waves were not detected in unlinked grafts. H_{max}/M_{max} values ranged between 5.324 at 0.5 mA stimulation and 0.076 at 19 mA stimulation, comparable to previously reported ranges[15]. Afferent signals on the antagonist nerve were produced in response to stimulation on the agonist nerve (Figure 3C) with magnitudes and latencies similar to those previously reported[7]. The afferent signals graded with the strain generated in the antagonist muscle (Figure 3D) – a direct result of proportionally coupled excursion. The main functionality of the AMI is to produce graded efferent and afferent signals in response to increasing agonist contraction. The electrophysiological results above confirmed that the AMIs created through a dual-stage process were capable of graded efferent and afferent with no significant difference from single-stage AMIs.

Force Production: Force feedback, via activation of Golgi tendon organs, is a critical component of the AMI. The ability for dual-stage AMIs to produce force was measured using a force gauge during electrical stimulation of the innervating nerves. Forces produced in the agonist muscle, ranged between 19.6 - 58.8 mN, and linearly correlated with stimulation amplitude and integrated EMG. Linear regression yielded an $r^2 = 0.86$ (Figure 4A). Integrated EMG and force production from a representative test is shown in Figure 4B. In their linear configuration, the regenerative AMIs had an electromechanical delay (between EMG production and force generation) of 59 +/- 7 ms on average. At lower amplitude stimulations (1 or 2mA), this delay was greater, ranging from 79-120 ms. This is consistent with ranges of skeletal muscle under concentric or eccentric contraction in humans[16,17].

Strain Generation: The primary component of afferent feedback is spindle activity, generated by strains in stretching muscle in response to agonist contraction. These grade with stimulation amplitude in regenerative AMIs[18]. Here, the addition of a separate surgical step did not adversely affect the strains produced by the regenerative AMI through excessive scarring. Strains in the agonist and antagonist are inversely proportional and represent proportionally coupled motion (Supplemental Figure. 3). The average strain was measured to be 10.7 +/- 3.07%. Control AMIs created through a single stage surgery performed with 8.1-18.2% strain, which is not significantly different from the experimental dual-stage group ($p = 0.05$). No coupled motion occurred in unlinked grafts in the negative control group as predicted.

Histological Results: Dual-stage AMIs were encapsulated in a collagenous fibrotic capsule. The tendon-tendon coaptation showed strong healing, with myocytes aligned isotropically near the region of coaptation and transitioning to collagenous tendon (Supplemental Figure. 4). The fascial layer between the AMI and biceps femoris measured

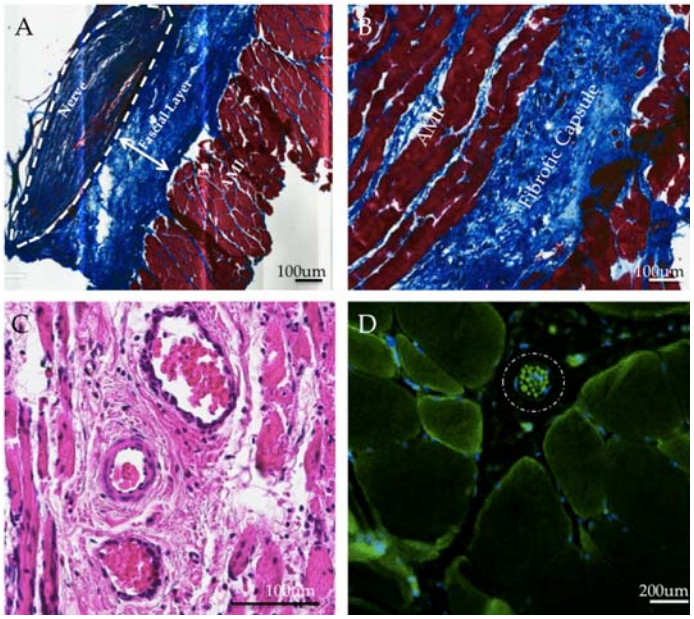

Figure 5. Histological Results. (A) Well-demarcated partition between the fascial layer and AMI. This slice captures a healthy collagen-bound nerve entering the muscle layer and reinnervating the muscle. (Trichrome stain) (B) The fibrotic capsule surrounding the upper layer of the AMI, through which new vessels formed, is comprised of loose, anisotropically oriented collagen. (Trichrome stain) (C) Well-epithelialized angiogenic vessels through scar bed facilitate revascularization. Surrounding musculatures appears healthy and mature. (H&E stain) (D) A spindle fiber (circled) is shown containing numerous intrafusal fibers between motor unit groups. (s46 stain)

176 +/-26 μm in the dual-stage (Figure 5A) AMI and 169 +/- 38 μm in single-stage controls, insignificant at the p = .05 level (t = .219 and a p= .413). The fibrotic capsule (Figure 5B) thickness measured 335 +/- 73 μm in dual-stage AMIs vs. 274 +/- 83 μm in single-stage controls, an insignificant difference (t= 1.25, p= .109). Collagen patterns and luxol fast blue staining demonstrated well-myelinated nerve branches spreading throughout the muscle. Muscle tissues were healthy and comprised of both regenerating myocytes and fully mature myocytes (Figure 5C). The average fiber thickness was 84 +/- 9 μm in AMI grafts and 89 +/- 7 μm in control grafts, an insignificant difference. In the second surgery, despite disruption of the scar bed through which angiogenesis occurred, both small capillaries and larger epithelialized vessels were formed throughout the graft, predominantly entering through the underlying scar bed. Blood vessels were found alongside the innervating nerves (Supplemental Figure. 5) and provided a non-disrupted vascular supply during the second transfer.

Alpha bungarotoxin staining revealed synaptogenesis, centered near the region at which the nerve was sutured into the muscle. Intrafusal spindle fibers are required for the transduction of critical fascicle length information for proprioceptive signaling. Muscle cross sections showed viable spindles with 6-16 intrafusal fibers each when stained with s46 (Figure 5D).

Discussion:

There are limited strategies to avail bidirectional efferent-afferent prosthetic control to persons with limb amputation. Of these, the AMI uniquely includes the provision of naturally-generated muscle-based proprioception[9]. The AMI effectively leverages regenerative grafts linked in an agonist-antagonist conformation, which lends itself to robust efferent and afferent signaling[7,10]. The isolation of end-target function in the AMI architecture make it particularly well-suited for prosthetic device control. In contrast, standard amputation and TMR require post-facto methods such as pattern recognition to identify the neural composition innervating end targets

Due to limitations of signal processing, pattern recognition has provided limited function for many patients, resulting in a low acceptance rate of pattern recognition-based devices[19,20]. Moreover, other amputation techniques such as TMR[19] and RPNI[14] employ no agonist-antagonist architecture and therefore do not provide the capacity for natural proprioception. The regenerative AMI is specifically apt for already amputated residua and can return lost functionality to those with standard amputations by providing bidirectional signaling capabilities[7].

Outcomes of the Dual-Stage Approach: The ability to create, resituate, and assemble regenerative peripheral nerve grafts is critical for the implementation and scaling of regenerative AMIs for multiple DOFs in

revision amputations. To emulate an amputation model, dissected branches of the sciatic nerve were placed into separate regenerative muscle grafts. Two weeks later (after identifying the function of each graft under stimulation), individual flexor and extensor grafts were paired. Mechanical, electrophysiological and histological evidence showed that a dual-stage surgery was viable in creating AMIs capable of graded afferent/efferent signaling at high SNRs. Strain rates, atrophy, and reinnervation were not negatively impacted by a dual-stage approach. Graded force production further validated the ability of the dual-stage AMI to overcome any limiting contractile conditions of the muscle, including elasticity/compliance constraints due to scarring and minimized fiber length[20].

Important Considerations for Revascularization: The disruption of vascular beds and added scarring through a second surgical stage proposed a significant viability concern in terms of vascularization. The revascularization of regenerative grafts occurs through a three-stage process: 1) plasmatic imbibition, 2) inosculation and capillary ingrowth, and 3) revascularization. Immediately following whole skeletal muscle graft transfer, diffusion-based imbibition comprises the primary mode of nutrient and chemical exchange. At 24 hours following grafting, previous studies have reported ischemic degeneration of large vessels within the muscle. Three to ten days post-operatively, new vessels grow through the scar bed into both old vessel lumens as well as newly formed channels[21]. In this study, 14 days post-operatively, grafts in the dual-stage experimental group were re-harvested, destroying any capillary ingrowth, restarting the revascularization process and potentially risking the viability of the grafts. However, both functional and histological results demonstrated insignificant differences between the control and experimental groups in terms of atrophy or myocyte morphology. Numerous small-diameter vessels were found growing centripetally through the scar bed to revascularize the graft. Moreover, it is likely that the blood vessels adjacent to the innervating nerve, which were not disrupted during the second surgery provided a vascular supply that helped mitigate ischemia during the second transfer. In addition, the angiogenic processes activated by the first transfer, consisting of various elevated mechanical, hormonal and metabolic components[22], remained active at the time of the second transfer and would have aided in the second revascularization cycle of the AMI.

Integrating with Reflexive Loops: In addition to validating a modular surgical approach for revising amputation limbs, this study demonstrated that regenerative muscle architectures are capable of recreating proprioceptive reflex loops. Given the recency of AMIs, that enable proprioceptive signaling through afferent neural pathways[7,10], there is a need to validate the presence and activity of reflexive loops in this architecture. Clinically, the Hoffman reflex (indicated by h-waves) is used to study motor circuits, muscle tone, conduction pathologies in

afferent axons, and diagnose peripheral neuropathies[23,24]. H-wave activity reflects the response of afferent fibers and reflex loops[15,25]. In this study, stimulation of effect nerves yielded h-waves for 7/10 grafts in the dual-stage AMI group. The amplitudes of these waves decreased as stimulation amplitude approached the supramaximal amplitude. This pattern is characteristic of healthy reflex loops. Lack of activity in certain grafts can be attributed to anesthetic states, varied recording electrode placement, and destructive interference of orthodromic and antidromic impulses due to stimulation electrode placement. Nevertheless, the integration of regenerative muscle grafts in natural reflexive loops indicates the ability of the regenerative AMI to be integrated into the natural/central nervous system, a newfound benefit of the AMI. This result is not only important for the amputation model, but also opens avenues for the creation of similar regenerative architectures to potentially manage afferent neuropathologies. Future work should focus on further characterizing the reflexive loops, especially in the 0-1mA stimulation range where they are gradually expected to increase in magnitude. Insights on the reflexive mechanisms enabled by the unique AMI architecture will play a role in the design of neuromuscular models operating on neuroprostheses that are used in consort with the AMI.

Mechanical Linkage Influencing Atrophy: This study additionally provides valuable insight in the use of agonist-antagonist pairs in potential prevention of disuse atrophy. In unlinked grafts, the high rate of atrophy (90%) compared to that of linked agonist-antagonist grafts (~50%), suggests that mechanical linkage strongly influences the process of atrophy. This may be potentially due to afferent signaling from reciprocal innervation, which promotes volitional use and consequent hypertrophy. This is not only important in the context of this surgery, but also in any surgeries or traumatic injuries where disuse atrophy ensues due to disruption of agonist-antagonist muscle pairs[26].

Translation to Amputation Surgery: For patients undergoing revision of a stump, this study presents a practical, technically feasible modular approach to assembling regenerative AMIs for each desired DOF (or transected nerve). These DOF can be controlled by an advanced bionic device using a controller calibrated to the signals generated from each muscle graft in the AMI [27]. In the worst-case scenario, where the identity of each nerve fascicle is uncertain, fascicular splits could be performed to divide as many fascicles as technically feasible. Each fascicle would then be placed inside a muscle graft and secured onto fascia, close to its estimated muscle pair. After reinnervation, the patient would be instructed to volitionally contract each muscle graft and identify its motor function. Each muscle graft would then be tagged using anatomical landmarks or injected fluoroscopic markers.

During a second surgery, the appropriate flexor-extensor pairs would be connected to form AMIs. If insufficient pairs or odd numbers of grafts existed, two small flexors could be connected to one extensor, based on function. For example, distinct branches of the tibial nerve innervate the plantaris and soleus, both of which help to plantarflex the ankle joint. Both flexor tendons could be connected to the extensor, the tibialis anterior, that dorsiflexes the ankle joint (Supplemental Figure. 6). Nerves for which corresponding DOFs are unavailable/undesired (fixators and synergistic muscles) in the prosthetic device could remain as isolated regenerative grafts in the residuum. In the best-case scenario, as in the case of a planned amputation, one or two natural agonist-antagonist pairs could be disinserted from the articulating joint and repositioned through a synovial canal around the bone, space permitting. Then, regenerative grafts could be created for other smaller nerves that were transected and connected to their known antagonists, or placed on superficial fascia for future action. By tailoring a combination of native and regenerative AMIs, each residuum could enable afferent signaling and improved controllability of a prosthetic device.

Considerations for Scale: Translation and implementation in humans will require a proportional scaling of the various components of this surgical approach, including graft size, surgical time course, and anatomical placement. In rats, we limited the size of the grafts to 150 mg, which has been reported to be the critical limit beyond which the surface area to volume ratio exceeds diffusional capabilities[22]. In humans, maximum free graft size has been reported to be 1cm x 4cm for similar applications[28]. Additionally, the time course of reinnervation in humans will occur on the order of months, instead of weeks. Coupled with post-surgical edema, scarring, wound healing, and other considerations, which limit a secondary operation within 60-90 days, we predict the second stage of surgery to take place between 3-6 months after the first in humans. Finally, the availability of superficial fascia and the shape of the residual limb will dictate the distance between grafts during the initial surgery.

Summary of Benefits: The regenerative AMI's direct integration with natural nervous-signaling circuits, isolation of target efferent signals with high SNR, scalability, and adaptability to a broad range of pre-existing anatomy make it a valuable method for stump revision. While the proposed dual-stage approach requires two separate surgical interventions, the outcomes of this study suggest that the associated risk of graft degeneration are fairly low and that the process results in an AMI with robust bidirectional signaling capabilities, potentially providing an improved functionality for patients with amputation. There is precedent in the literature and practice for various multi-step surgeries, including sympathectomies[29], tumor resections[30], fistula corrections[31], and hip

replacements[32]. Further, previous studies demonstrate that revision surgery in persons with amputation often promotes favorable outcomes including pain relief and improved motor function[3,33].

Despite the volume of patients suffering from stump-related problems, there are few standardized protocols for stump revision and functional restoration[34]. This study offers a practical, technically feasible surgical strategy for implementing the regenerative AMI through a dual-stage method to revise amputated residua and return lost nerve function for at least some, if not all, terminal nerves. This work represents a step towards restoration of natural dynamic functionality, allowing persons with amputation to benefit from an improved prosthetic control and natural proprioceptive feedback.

Acknowledgements
We thank Hyun-Geun Song, Matt Weber, Tyler Clites, and Peter Calvaresi for technical assistance and the Koch Institute Swanson Biotechnology Center for their technical support with histology. This work was funded by the MIT Media Lab Consortia.

Data Availability
The datasets generated during and/or analyzed during the current study are available from the corresponding author on reasonable request.

Author Contributions:
S.S. designed the study, performed the surgeries, data collected and analysis and wrote the manuscript. M.D. contributed to data collection, analysis and writing of the manuscript. M.C and H.H provided intellectual guidance and contributed to writing the manuscript.

Competing interests
The author(s) declare no competing interests.

References

1. Kumar, D. *et al.* Need of Revision of Lower Limb Amputations in a North Indian Tertiary Care Centre. *J. Clin. Diagn. Res. JCDR* **9,** RC01–RC03 (2015).
2. Sehirlioglu, A. *et al.* Painful neuroma requiring surgical excision after lower limb amputation caused by landmine explosions. *Int. Orthop.* **33,** 533–536 (2009).
3. Bourke, H. E., Yelden, K. C., Robinson, K. P., Sooriakumaran, S. & Ward, D. A. Is revision surgery following lower-limb amputation a worthwhile procedure? A retrospective review of 71 cases. *Injury* **42,** 660–666 (2011).
4. Themes, U. F. O. Lower Extremity Assessment Project (LEAP) – The Best Available Evidence on Limb-Threatening Lower Extremity Trauma. *Musculoskeletal Key* (2017).
5. Irwin, Z. T. *et al.* Chronic recording of hand prosthesis control signals via a regenerative peripheral nerve interface in a rhesus macaque. *J. Neural Eng.* **13,** 046007 (2016).
6. Cheesborough, J. E., Smith, L. H., Kuiken, T. A. & Dumanian, G. A. Targeted Muscle Reinnervation and Advanced Prosthetic Arms. *Semin. Plast. Surg.* **29,** 62–72 (2015).

7. Srinivasan, S. S. *et al.* On prosthetic control: A regenerative agonist-antagonist myoneural interface. *Sci. Robot.* **2,** eaan2971 (2017).
8. Riemann, B. L. & Lephart, S. M. The Sensorimotor System, Part II: The Role of Proprioception in Motor Control and Functional Joint Stability. *J. Athl. Train.* **37,** 80–84 (2002).
9. Clites, T. R. *et al.* Proprioception from a Neurally-Controlled Bionic Prosthesis. *Sci. Transl. Med.* doi:in press
10. Clites, T. R., Carty, M., Srinivasan, S., Zorzos, A. & Herr, H. A murine model of a novel surgical architecture for proprioceptive muscle feedback and its potential application to control of advanced limb prostheses. *J. Neural Eng.* (2017). doi:10.1088/1741-2552/aa614b
11. Singson, R. D. *et al.* Postamputation neuromas and other symptomatic stump abnormalities: detection with CT. *Radiology* **162,** 743–745 (1987).
12. O'Reilly, M. A. R. *et al.* Neuromas as the cause of pain in the residual limbs of amputees. An ultrasound study. *Clin. Radiol.* **71,** 1068.e1-1068.e6 (2016).
13. Daniilidis, K., Stukenborg-Colsman, C. M., Ettinger, M. & Windhagen, H. Huge sciatic neuroma presented 40 years after traumatic above knee amputation. *Technol. Health Care* **21,** 261–264 (2013).
14. Kung, T. A. *et al.* Regenerative peripheral nerve interface viability and signal transduction with an implanted electrode. *Plast. Reconstr. Surg.* **133,** 1380–1394 (2014).
15. Cliffer, K. D. *et al.* Consistent repeated M- and H-Wave recording in the hind limb of rats. *Muscle Nerve* **21,** 1405–1413 (1998).
16. Cavanagh, P. R. & Komi, P. V. Electromechanical delay in human skeletal muscle under concentric and eccentric contractions. *Eur. J. Appl. Physiol.* **42,** 159–163 (1979).
17. Johns, G., Morin, E. & Hashtrudi-Zaad, K. The role of electromechanical delay in modelling the EMG-force relationship during quasi-dynamic contractions of the upper-limb. in *2016 38th Annual International Conference of the IEEE Engineering in Medicine and Biology Society (EMBC)* 3634–3637 (2016). doi:10.1109/EMBC.2016.7591515
18. Srinivasan, S. S. *et al.* On prosthetic control: A regenerative agonist-antagonist myoneural interface. *Sci. Robot.* **2,** eaan2971 (2017).
19. Kuiken, T. A., Marasco, P. D., Lock, B. A., Harden, R. N. & Dewald, J. P. A. Redirection of cutaneous sensation from the hand to the chest skin of human amputees with targeted reinnervation. *Proc. Natl. Acad. Sci.* **104,** 20061–20066 (2007).
20. Roberts, T. J. & Gabaldón, A. M. Interpreting muscle function from EMG: lessons learned from direct measurements of muscle force. *Integr. Comp. Biol.* **48,** 312–320 (2008).
21. White, T. P. & Devor, S. T. Skeletal muscle regeneration and plasticity of grafts. *Exerc. Sport Sci. Rev.* **21,** 263–295 (1993).
22. Hudlicka, O., Brown, M. & Egginton, S. Angiogenesis in skeletal and cardiac muscle. *Physiol. Rev.* **72,** 369–417 (1992).
23. Kai, S. & Nakabayashi, K. Evoked EMG Makes Measurement of Muscle Tone Possible by Analysis of the H/M Ratio. (2013). doi:10.5772/55783
24. Burke, D. Clinical uses of H reflexes of upper and lower limb muscles. *Clin. Neurophysiol. Pract.* **1,** 9–17 (2016).
25. Palmieri, R. M., Ingersoll, C. D. & Hoffman, M. A. The Hoffmann Reflex: Methodologic Considerations and Applications for Use in Sports Medicine and Athletic Training Research. *J. Athl. Train.* **39,** 268–277 (2004).
26. Lundy-Ekman, L. *Neuroscience - E-Book: Fundamentals for Rehabilitation*. (Elsevier Health Sciences, 2013).
27. Clites, T. R. *et al.* Proprioception from a neurally controlled lower-extremity prosthesis. *Sci. Transl. Med.* **10,** eaap8373 (2018).
28. Cederna, P. S. RPNI - Human Trials. (2016).
29. Ibrahim, M. *et al.* Two-stage unilateral versus one-stage bilateral single-port sympathectomy for palmar and axillary hyperhidrosis. *Interact. Cardiovasc. Thorac. Surg.* **16,** 834–838 (2013).
30. Hida, K., Iwasaki, Y., Seki, T. & Yano, S. two-stage operation for resection of spinal cord astrocytomas: technical case report of three cases. *Neurosurgery* **58,** ONS-E373; discussion ONS-E373 (2006).

31. Shin, H. K., Choi, C. W., Lim, J. W. & Her, K. Two-stage Surgery for an Aortoesophageal Fistula Caused by Tuberculous Esophagitis. *J. Korean Med. Sci.* **30,** 1706–1709 (2015).

32. Wolf, M. *et al.* Prosthetic joint infection following total hip replacement: results of one-stage versus two-stage exchange. *Int. Orthop.* **38,** 1363–1368 (2014).

33. Liu, K., Tang, T., Wang, A. & Cui, S. Surgical revision for stump problems after traumatic above-ankle amputations of the lower extremity. *BMC Musculoskelet. Disord.* **16,** 48 (2015).

34. Baumgartner, R. & Riniker, C. Surgical Stump Revision as a Treatment of Stump and Phantom Pains: Results of 100 Cases. in *Phantom and Stump Pain* 118–122 (Springer, Berlin, Heidelberg, 1981). doi:10.1007/978-3-642-68264-3_19

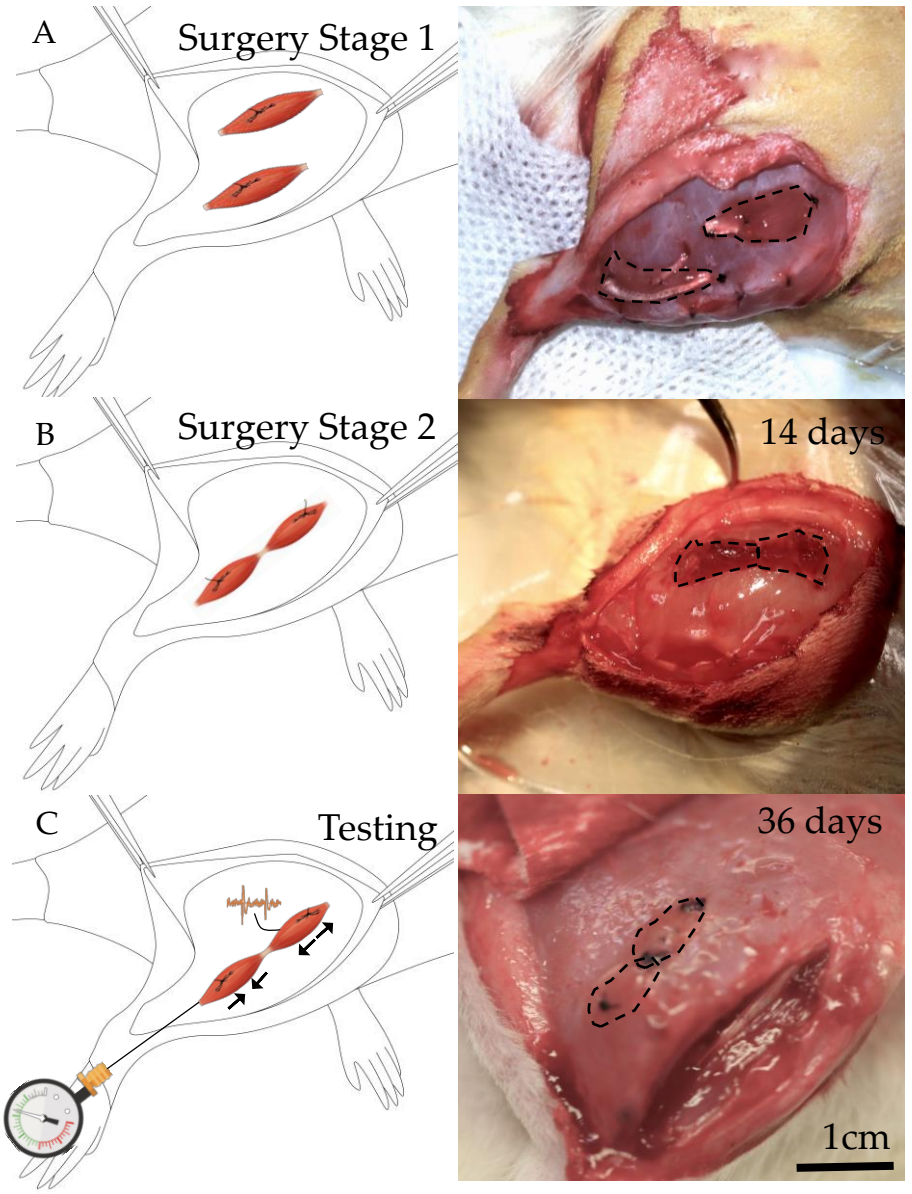
A
Surgery Stage 1
B
Surgery Stage 2
14 days
C
Testing
36 days
1cm

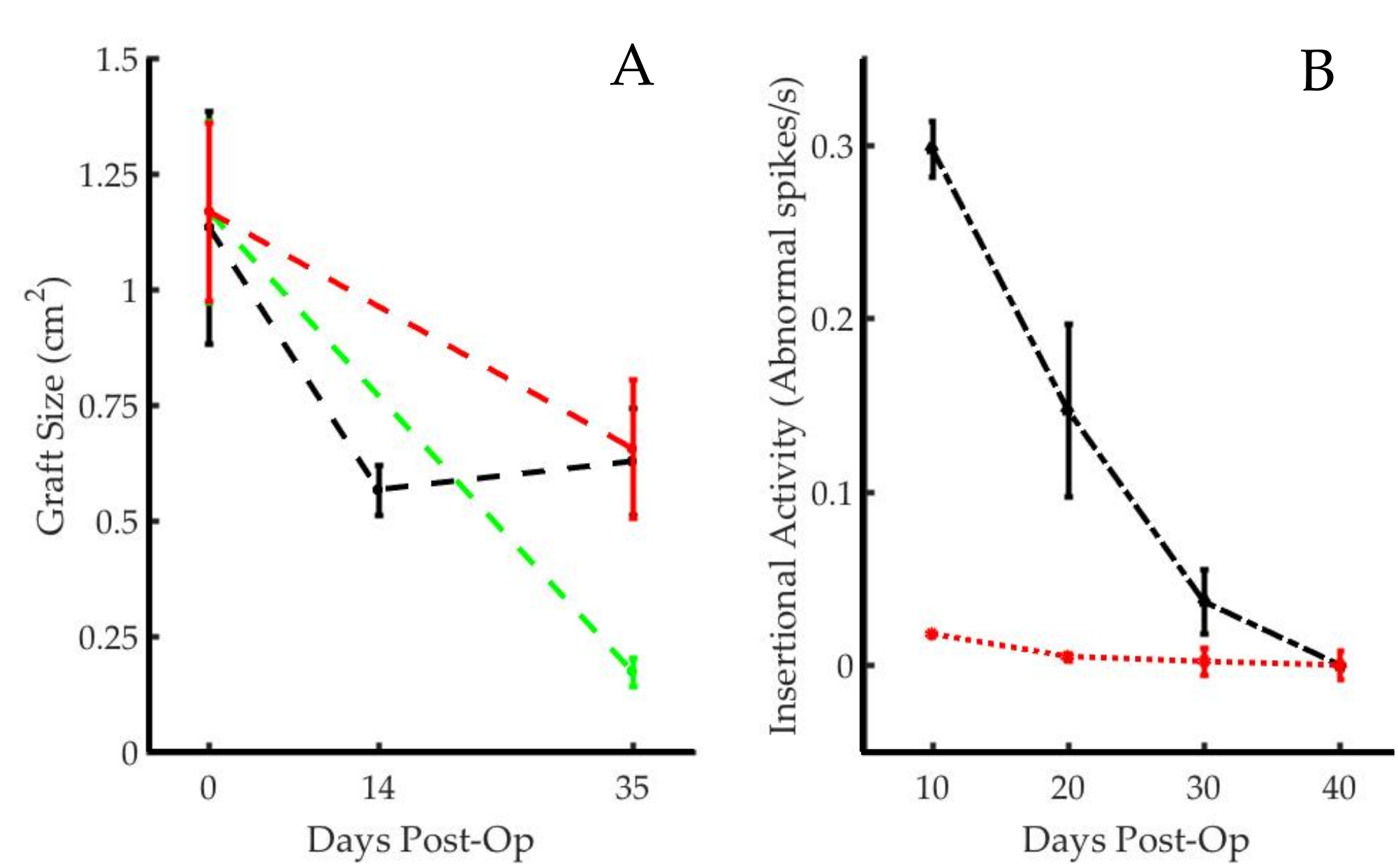
A
B
1.5
1.25
1
0.75
0.5
0.25
0
Graft Size (cm^2)
0
14
35
Days Post-Op
0.3
0.2
0.1
0
Insertional Activity (Abnormal spikes/s)
10
20
30
40
Days Post-Op

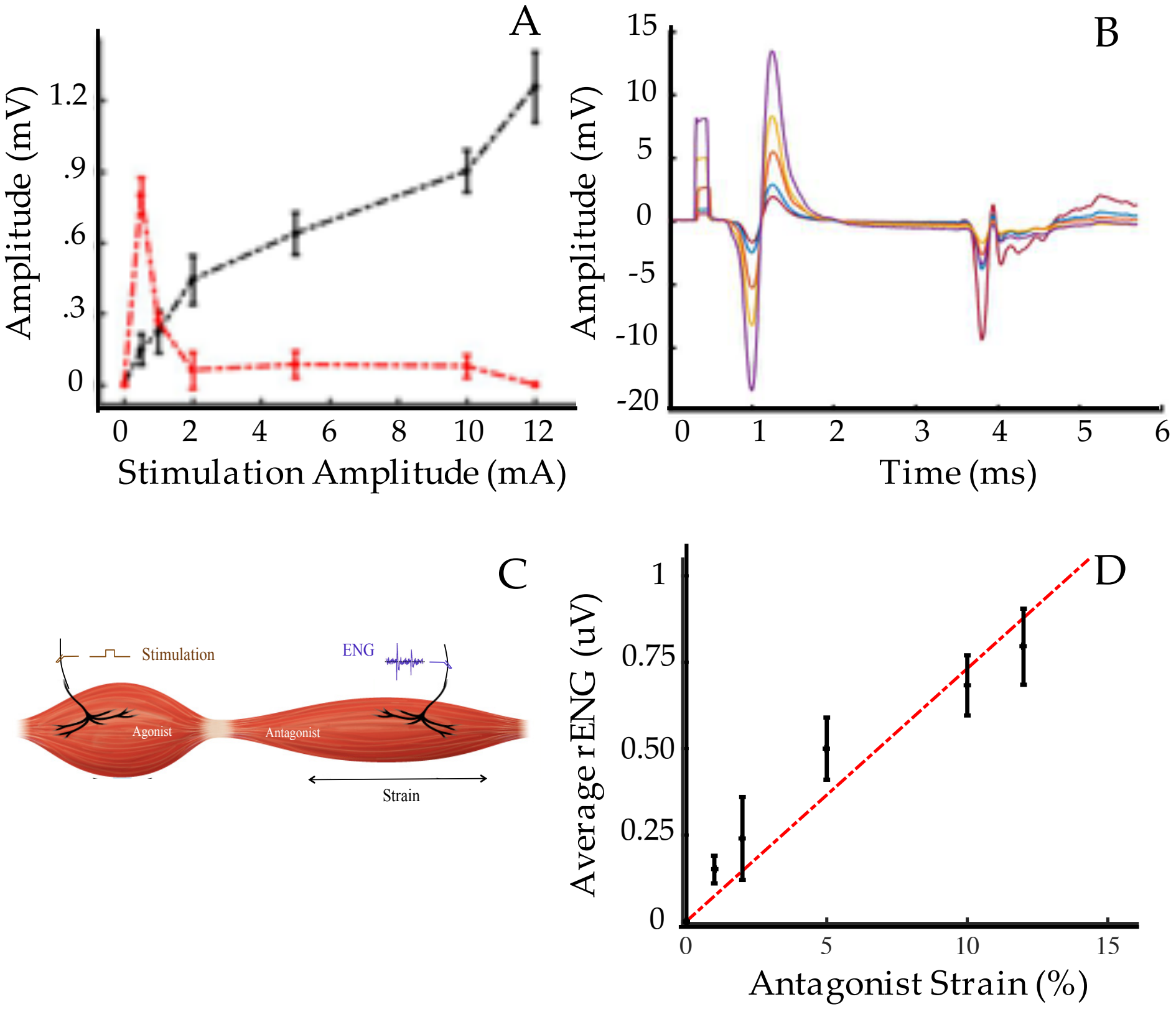
A
Amplitude (mV)
1.2
.9
.6
.3
0
0
2
4
6
8
10
12
Stimulation Amplitude (mA)
B
Amplitude (mV)
15
10
5
0
-5
-10
-20
0
1
2
3
4
5
6
Time (ms)
C
Stimulation
ENG
Agonist
Antagonist
Strain
D
Average rENG (uV)
1
0.75
0.50
0.25
0
0
5
10
15
Antagonist Strain (%)

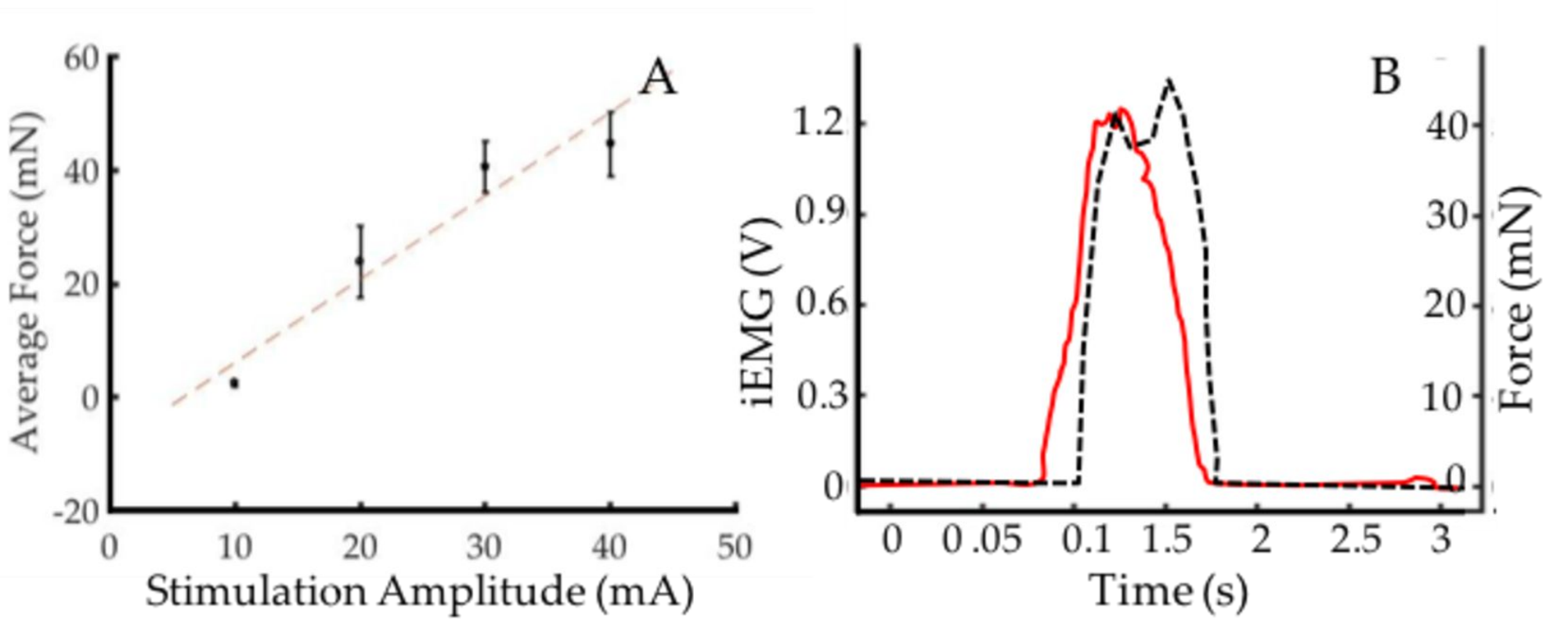
A
Average Force (mN)
60
40
20
0
-20
0
10
20
30
40
50
Stimulation Amplitude (mA)
B
iEMG (V)
1.2
0.9
0.6
0.3
0
Force (mN)
40
30
20
10
0
0
0 .05
0.1
1.5
2
2.5
3
Time (s)

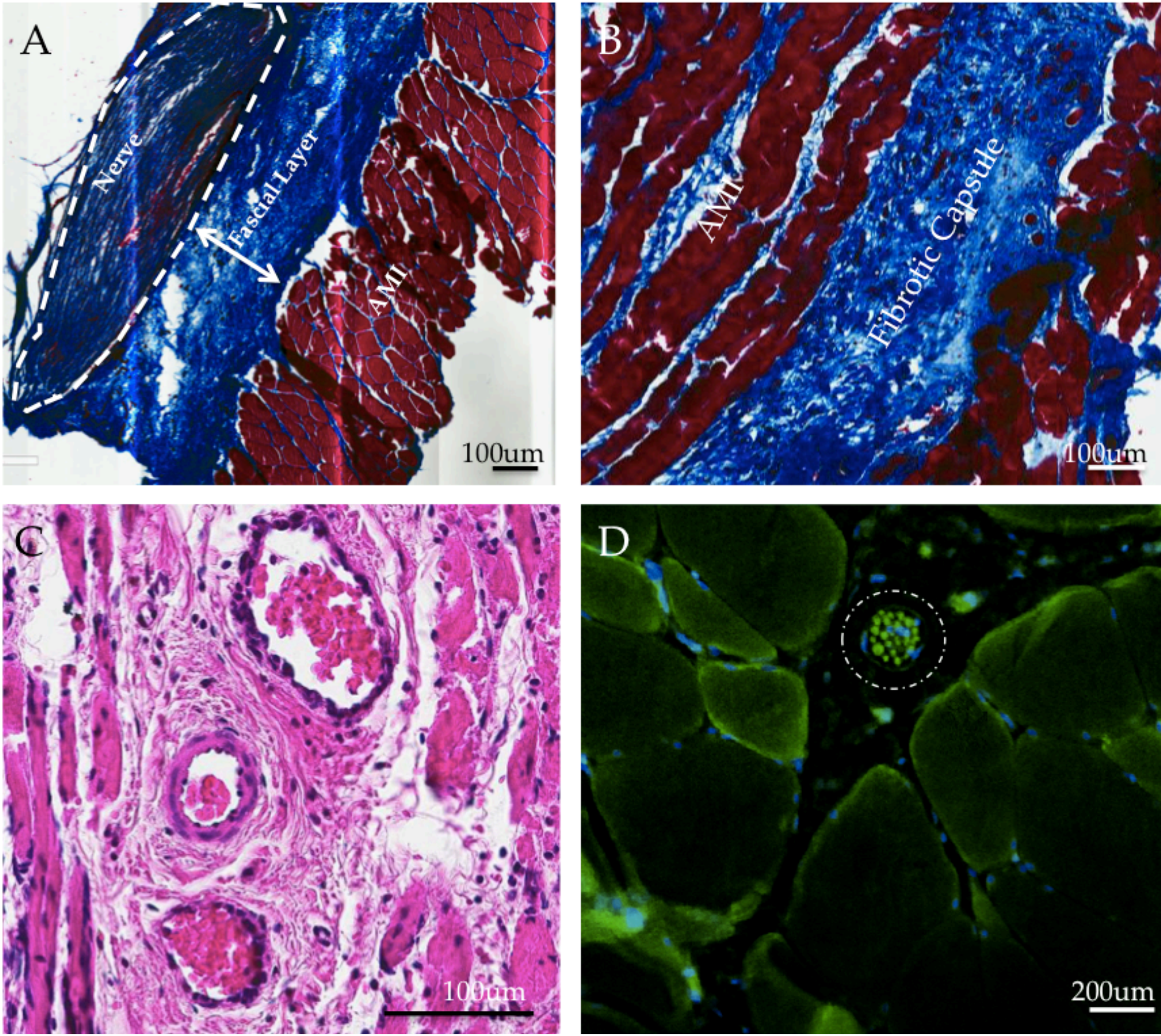
A
Nerve
Fascial Layer
AMI
100um
B
AMI
Fibrotic Capsule
100um
C
100um
D
200um